

# Self-Healing Polyurethanes with Shape Recovery

Yunseon Heo and Henry A. Sodano\*

Two new thermoresponsive self-healing polyurethanes (1DA1T and 1.5DA1T) based on the Diels–Alder (DA) reaction between furan and maleimide moieties are developed that use the shape-memory effect to bring crack faces into intimate contact such that healing can take place. Unlike other self-healing polymers, these polymers do not require external forces to close cracks but rather they use the shape-memory effect to autonomously close the crack. Both polyurethanes have a stable polymer structure and comparable mechanical properties to commercial epoxies. A differential scanning calorimeter is employed to check the glass transition temperature of the polymers as well as the DA and retro-DA (rDA) reaction temperatures. These DA and rDA reactions are confirmed with variable-temperature proton nuclear magnetic resonance. Healing efficiency is calculated using a measurement of the failure load from compact tension testing. The results show that the shape-memory effect can replace external forces to close two crack surfaces and the DA reaction can be repeatedly employed to heal the cracks.

## 1. Introduction

The development of self-healing polymers has grown over the past decade due to their ability to repair damage occurring before complete failure. Current methods have allowed for the development of self-healing polymers that are able to achieve strong healing performance, but the healing process for these polymers are either not inherently repeatable (i.e., a capsule based<sup>[1]</sup> and a vascular based)<sup>[2]</sup> or require the use an external pressure to close the crack and bring the surfaces into contact.<sup>[3–5]</sup> While many promising self-healing methods are under development, to date, polymers that utilize the Diels–Alder (DA) reaction have been the most promising since it is highly efficient, simple and can be repeatedly healed through only the application of heat.

The Diels–Alder (DA) reaction is a thermally reversible reaction between a conjugated diene and a dienophile resulting in a cyclohexene derivative.<sup>[6]</sup> The crosslinked DA adducts can undergo a reverse reaction at higher temperatures which is known as a retro Diels–Alder (rDA) reaction.<sup>[7]</sup> Chen et al. determined the new  $\sigma$  bond energy between a furan and maleimide

of the DA adduct with differential scanning calorimetry (DSC). The bond energy of the new C–C  $\sigma$  bond in the DA adducts was 96.2 kJ/mol<sup>[3]</sup> while other covalent bond energies are 348 kJ/mol for C–C bonding, 293 kJ/mol for C–N bonding, and 389 kJ/mol for N–H bonding.<sup>[8]</sup> This implies that covalent bonds are at least 3 to 4 times stronger than the intermolecular C–C  $\sigma$  bond between the DA adducts. Therefore, cracks are more likely to propagate through new C–C  $\sigma$  bonds than the other bonds. Consequently, healing is possible on the crack surfaces through the recovery of broken DA crosslinks and the healing efficiency directly correlates to the crosslink recovery. The temperature ranges for the DA and rDA reactions are also advantageous. The DA reaction occurs at temperatures between room temperature and approximately 90 °C

without any other external stimulus.<sup>[9]</sup> Thus, DA polymers can still counteract the propagation of micro-damage at ambient temperature. Also, the range for the rDA reaction is approximately 130 °C which is low enough to avoid thermal degradation of the polymer upon heating and high enough for many applications<sup>[9]</sup> such as a structural composite or electronic device coating materials.

When considering self-healing polymers with the DA reaction, the major limitation of the current healing processes is the need for external forces to bring the two crack surfaces together. It is believed that the shape memory effect from shape memory polymers (SMPs) can replace the use of external force. SMPs are a group of polymers that have the capability of recovering their permanent shape upon the application of an external stimulus, even after significant deformation.<sup>[10]</sup> This is possible due to what is known as the shape memory effect.

An advantage of SMPs is their versatility since they can be synthesized to have a wide range of properties depending on its chemical structures and compositions.<sup>[11]</sup> According to Lendlein et al., the shape memory effect arises from the combination of the structure and morphology of the polymers. In SMPs, two notable features exist; a soft segment (switching segment) and a hard segment (netpoint).<sup>[12]</sup> The temporary shape of an SMP is fixed in a soft segment that consists of the chains, while the permanent shape is memorized in a hard segment that can consist of covalent bonds or intermolecular interactions.<sup>[10,12,13]</sup>

Recently, Rodriguez et al.<sup>[14]</sup> and Luo and Mather<sup>[15]</sup> reported shape memory assisted self-healing polymers (SMASH). In both papers, the shape memory properties originated from the covalent bonds (a hard segment); the network poly( $\epsilon$ -caprolactone)<sup>[14]</sup> and the epoxy matrix<sup>[15]</sup> and the healing mechanism was due to the diffusion of PCL which is a thermoplastic

Y. Heo, Dr. H. A. Sodano  
Materials Science and Engineering  
University of Florida  
Gainesville, FL 32611, USA  
E-mail: hsodano@ufl.edu

Dr. H. A. Sodano  
Mechanical and Aerospace Engineering  
University of Florida  
Gainesville, FL 32611, USA



DOI: 10.1002/adfm.201400299

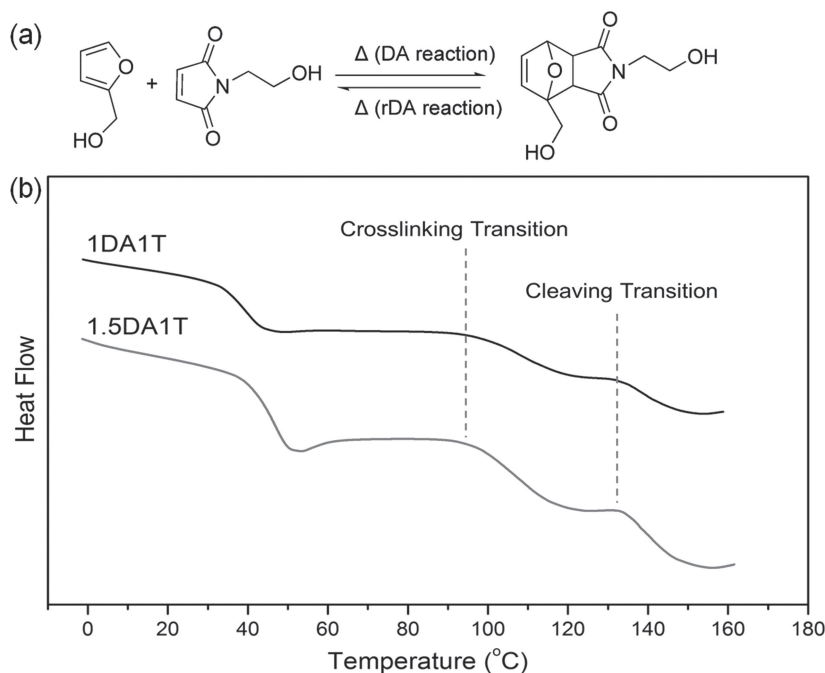


**Figure 1.** (a) The mechanism for the reversible DA reaction of FA and HEM, and (b) DSC data for polyurethanes (1DA1T and 1.5DA1T with FA, HEM, TEA, and HDI).

polyester with a relatively low melting point below 60 °C.<sup>[16]</sup> Thus, in both works, two different types of polymers; shape memory type and thermoplastic PCL, were blended and PCL were melted and flowed to heal the surfaces after closing the cracks using the shape memory effect. One of the biggest drawbacks of these SMASHs results due to the low melting point of PCL, the applicable temperature ranges are thus limited to below 60 °C. However, in this work, the synthesized polymers are applicable up to 130 °C before the C–C  $\sigma$  bonds cleave and are thermally stable up to 250 °C. Also, they combine both self-healing and shape memory properties such that no external forces are required to heal the crack. In order to increase stability while maintaining good mechanical properties, a thermoset polyurethane polymer system was chosen and the previously published shape memory polyurethane by Wilson et al.<sup>[13]</sup> was adapted into the developed polymers with the DA self-healing mechanism to create one complete polymer network. This has allowed for more in depth testing and characterization on the self-healing property in this work. All DA monomers were designed to connect to the polyurethane's main chain and as a result, the DA monomers require a hydroxyl functional group such that they can react with the isocyanate functional groups to form polyurethane.

## 2. Results and Discussion

### 2.1. Synthesis of Polymers

Commercial furfuryl alcohol (FA) and synthesized *N*-(2-hydroxyethyl)-maleimide (HEM) were employed for the self-healing property through the DA reaction and triethanolamine

(TEA) and hexamethylene diisocyanate (HDI) were adapted for the shape memory properties.<sup>[13]</sup> The polyurethanes that were synthesized for testing consisted of 1 mole of DA monomer (precrosslinked FA and HEM), 1 mole of TEA, and 2.5 mole of HDI for 1DA1T polymer and 1.5 mole of DA monomer, 1 mole of TEA and 3 moles of HDI for 1.5DA1T. The detailed syntheses procedures for the HEM which are similar to the method employed by Heath et al.<sup>[17]</sup> and the polymerization method and the polyurethane structure scheme can be found in the Experimental Section.

### 2.2. Thermal Analysis of the Diels–Alder Reaction

The mechanism for the reversible DA reaction between FA and HEM is shown in Figure 1a and the temperature ranges of crosslinking and cleaving in polymers were studied using DSC as shown in Figure 1b. From the DSC data, the average transition temperatures are obtained and shown in Table 1. The average glass transition temperature (42.4 °C for 1DA1T and 45.6 °C for 1.5DA1T) of the polymers are shown in the first transition in Figure 1b. Also, the second and third transitions in Figure 1b indicate the crosslinking temperature (the average of 97.3 °C for 1DA1T and 96.6 °C for 1.5DA1T) and the cleaving temperature (the average of 131.6 °C for 1DA1T and 129.3 °C for 1.5DA1T) and these transition temperatures in two different polymers are very similar showing for the reversible DA reaction between FA and HEM monomers in the polyurethane network. Moreover, they seem slightly higher when compared to the reported DA and rDA reaction temperatures (i.e., 93 °C and 120 °C,<sup>[4]</sup> respectively). This can be attributed to the requirement for additional thermal energy to overcome the bonding energies between all the molecules in the polymer such that the molecules become sufficiently mobile, showing that these polymers network are very stable.

### 2.3. Reversibility of the Diels–Alder and Retro Diels–Alder Reactions

Variable temperature proton nuclear magnetic resonance (VT NMR) was used to confirm the reversible DA reaction. VT NMR was a better tool to analyze the actual amount of the DA reversibility since this reaction is temperature dependent, and the bonding information, especially of the cleaved bonding, could be acquired at the reaction temperatures. With traditional NMR, a specimen after cleaving would need to be immediately quenched down to a lower temperature and kept at a low temperature to maintain the cleaved bonds. Otherwise some crosslinking due to the sample being at an ambient temperature could occur, meaning that the cleaving NMR data are not

**Table 1.** The average glass transition temperature, crosslinking temperature, and cleaving temperature and their standard deviations for 1DA1T and 1.5DA1T.

	1DA1T	Standard Deviation	1.5DA1T	Standard Deviation
Glass Transition Temperature [°C]	42.4	2.06	45.6	3.77
Crosslinking Temperature [°C]	97.3	2.45	96.6	1.53
Cleaving Temperature [°C]	131.6	2.66	129.3	2.48

representative of what actually occurs at cleaving temperatures. Thus, VT NMR is better for investigating the amount of the cleaved bonds and their reversibility. Moreover, the crosslinking and cleaving times can be estimated by repeatedly scanning the peaks until the reactions are complete. These recorded reaction times and temperatures were then used to design the healing process.

For the VT NMR testing, the precrosslinked DA monomers were tested as a model system to evaluate the feasibility of the crosslinking/cleaving reactions between HEM and FA monomers that have the healing property in the polymers. First, the sample was kept at 140 °C for 30 min for the cleaving process (Figure 2a) and then cooled down to 80 °C for 120 min for the crosslinking DA reaction (Figure 2b). To confirm the repeatability of the reactions, the sample was re-heated to 140 °C and kept at this temperature for 30 min (Figure 2c) and finally re-cooled down to 80 °C for 120 min for crosslinking DA reaction (Figure 2d). As clearly shown in Figure 2b and d, two peaks at 6.52 ppm and 5.08 ppm appear as HEM and FA monomers are connected at 80 °C. These peaks were identified from the NMR data of the HEM monomer synthesis comparing the product (2) and HEM in the Experimental Section and the actual NMR peaks are also attached in Figure S3 and Figure S5 in the Supporting Information. As furan is removed from product (2), the 6.52 ppm and 5.08 ppm peaks disappear in the NMR data, meaning that these peaks indicate the new  $\sigma$  bond was created

through the DA reaction. Then, as shown in Figure 2a and c, the two peaks disappear as the temperature increases to 140 °C since the crosslinked HEM and FA monomers become disconnected. These four NMR spectra indicate that the DA reaction occurs repeatedly between the HEM and FA monomers. The residue peaks of the new  $\sigma$  bonds still appear for the cleaved cases (shown in Figure 2a and c) even though the specimen and solvent in the NMR tube was kept at 140 °C until the peaks did not show any changes. This indicates that the rDA reaction is not 100% efficient, meaning that the DA and rDA reversibility was not 100% effective.

## 2.4. Self-Healing Efficiency

The healing performance shape memory polymers were evaluated through fracture testing. Compact tension (CT) tests were performed on an Instron 5969 to measure the peak load to induce fracture in the glassy state of the as cast and healed specimens. CT test specimens with a pin-pin configuration and slightly modified dimensions from the ASTM D 5045 standard were constructed using a computer numerical control (CNC) mill with the dimensions shown in Figure 3a. The first modification of the ASTM dimensions was the addition of a resting hole along the crack path to terminate the propagation in the middle of the sample. This was needed since the shape memory effect will arise from the portion of the sample that is left in tact and the polymers exhibit uncontrolled crack growth in its glassy state. In addition, the notch length was shortened to enhance the shape memory effect. Using the initial and post healing maximum loads that were acquired through the use of CT testing, the healing efficiency was calculated using Equation (1).<sup>[18]</sup>

$$\text{Healing Efficiency (\%)} = \frac{\text{Max.Load}_{\text{healed}}}{\text{Max.Load}_{\text{initial}}} \times 100 \quad (1)$$

Figure 3c and d show the CT test results for 1DA1T and 1.5DA1T polymer samples. The average healing efficiencies were calculated with the fracture loads from 6 specimens for 1DA1T and 8 specimens for 1.5DA1T. More 1.5DA1T specimens were tested for the statistical stability since 1.5DA1T polymer data had larger variations. For the first, second, and third healing processes, the efficiencies of 79.76%, 69.30%, and 59.26% for 1DA1T and 84.08%, 84.34%, and 75.89% for 1.5DA1T, respectively, were calculated and the error bars as shown in Figure 3b indicate the standard deviation of multiple specimens. The 1.5DA1T polymer efficiencies show the higher and more stable healing efficiency compared to them of 1DA1T due to the amount of available furan and maleimide molecules to heal the crack surfaces.

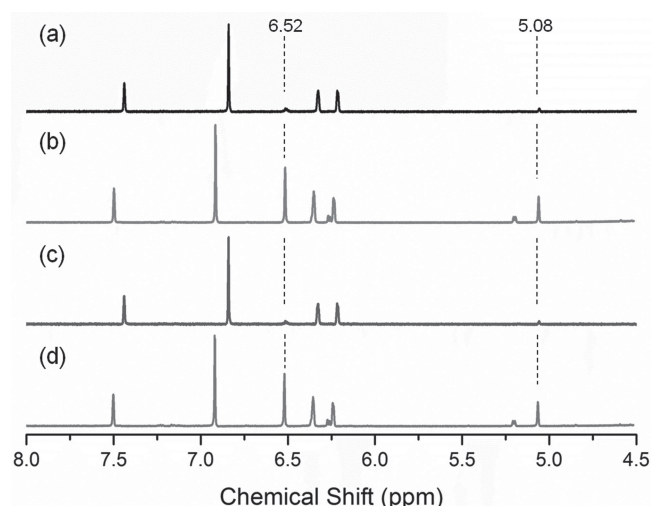


**Figure 2.** VT NMR data for HEM and FA precrosslinked monomer to see the Diels–Alder reversibility; the precrosslinked monomer was (a) kept at 140 °C for 30 min (cleaving, rDA reaction), (b) cooled down to 80 °C for 120 min (crosslinking, DA reaction), (c) heated up to 140 °C for 20 min (cleaving, rDA reaction), and (d) cooled to 80 °C for 120 min (crosslinking, DA reaction)

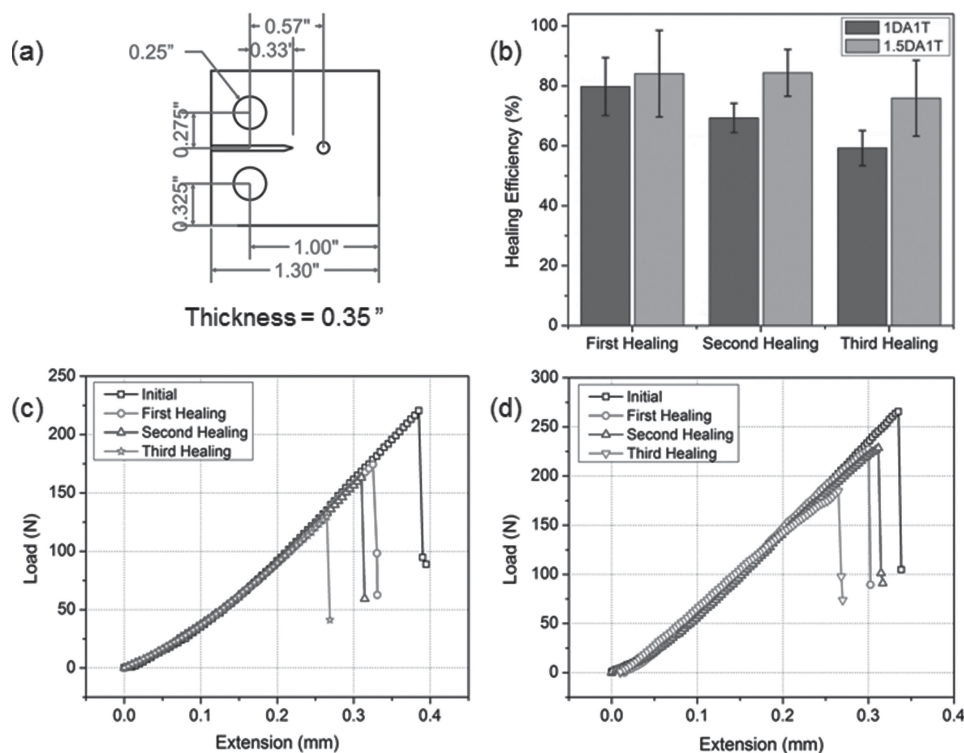


**Figure 3.** (a) Dimension of a compact tension test specimen (unit in inches) with a thickness of 0.35", (b) the average healing efficiencies of 1DA1T and 1.5DA1T for the first, second and third healing (79.76%, 69.30%, and 59.26% for 1DA1T and 84.08%, 84.34%, and 75.89% for 1.5DA1T), (c) 1DA1T example plot of failure loads as a function of extension (showing healing efficiencies of 79.15%, 73.99%, and 58.77% for the first, second and third healing, respectively), and (d) 1.5DA1T example plot of failure loads as a function of extension (showing healing efficiencies of 85.59%, 86.12%, and 69.60% for the first, second, and third healing, respectively).

The measured healing efficiency is approximately 80–85% of the virgin fracture load. There are two primary reasons for the efficiency falling below 100%, the first is a result of the efficiency of the re-crosslinking reaction of the DA molecules and the second being related to the sharpening of the crack tip due to fracture is the virgin sample. For the crack to completely heal the polymer network needs to be completely reformed; however, it is probable that following healing disconnected molecule pairs exist in the specimen. As shown in the VT NMR data (Figure 2), the cleaving process (rDA reaction) is not 100% effective in solution and is expected to be lower in the solid state due to steric effects, which may result in diminished healing efficiency. A second explanation is that the healing mechanism is also difficult to accurately measure since the crack in the healed specimens will always be sharper than the pre-crack produced in the virgin sample and thus higher stress intensity should exist following healing. This higher stress intensity would produce an apparent rather than true reduction in healing efficiency. The influence of this factor could be reduced through the formation of a starter crack by creating a stable crack growth process, however this was challenging with the glassy polymer and efforts to accomplish this were unsuccessful. Each of these reasons for the incomplete efficiency gradually reduces the healing efficiency with increasing healing cycles. However, both the 1DA1T and 1.5DA1T polymers possess superior healing efficiencies when compared (using

fracture strength) to similar polymers calculated the and seen in the literature, including 2MEP4F<sup>[4]</sup> and polymer 400<sup>[19]</sup> with reported average first healing efficiencies of 80% and 46%, respectively.

## 2.5. Healing Process

The temperature profile for the healing process was designed to have enough time to crosslink and cleave based on the VT NMR data. After a crack was formed in the specimens and without the use of an external force to close the crack, the CT specimens were placed face-down in a vacuum oven under a nitrogen environment such that no gravitational forces contributed to the crack closure. The oven was slowly heated up to 135 °C over 2.5 h and kept at this temperature for 2 h. Then, the specimens were cooled down to 90 °C over 1 h and kept at this temperature for 2 h and finally cooled to 70 °C over 1 h and kept again at this temperature for another 2 h. The specimens were heated up to a temperature above the cleaving temperature so that the unbroken bonds could separate into two individual molecules. This allowed for a greater chance to heal the cracks when undergoing the DA reaction since polymer cannot return the crack faces into its exact prior condition to allow the formation of identical bonds. Also, 2 h rest steps were taken at 90 °C and 70 °C since the gradual temperature changes ensured that the specimens were cooled



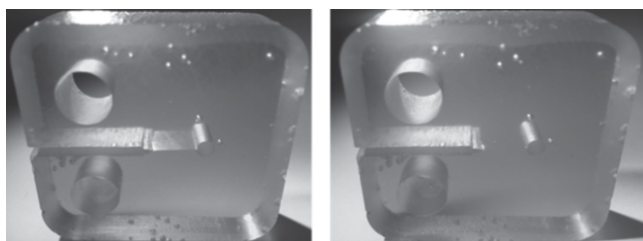


**Figure 4.** Image of a specimen after cracking (left) and after the thermal healing process without the use of external forces (right).

uniformly. **Figure 4** shows a cracked specimen before (left) and the same specimen after the thermal healing process (right).

## 2.6. Shape Memory Property of the Polymer

Shape memory polyurethanes were adapted from the previously published work by Wilson et al. and their shape memory properties were confirmed by the cyclic tensile testing.<sup>[13]</sup> However, in order to evaluate the shape memory property of 1DA1T and 1.5DA1T, the recovery capability tests in two different directions under free-strain conditions were conducted and the representative results for 1.5DA1T are shown in **Figure 5**. **Figure 5a** shows the permanent shape (dimensions of 48.6 mm × 8.73 mm × 1.08 mm) and **Figure 5b** presents the temporary shape after heating the film for 100 °C for 5 min, stretching the film, and then cooling it down to room temperature in order to fix the shape. Finally, **Figure 5c** displays the recovered permanent shape after heating the sample to 100 °C, which is above the glass transition temperature. An additional test was performed to show the spiral shape memory property of the polymer. **Figure 5d** shows the permanent shape (dimensions of 76.5 mm × 8.6 mm × 1.06 mm) and **Figure 5e** exhibits the coiled temporary shape at room temperature after heating the film at 100 °C for 5 min and fixing it. Lastly, **Figure 5f** illustrates the permanent shape of the polymer after recovery. Through these tests, it can be concluded that the developed self-healing polyurethanes contain shape recovery and this shape recovery force can be used to close the crack with the application of heat during the healing process.

## 2.7. Mechanical Properties of the 1DA1T and 1.5DA1T Polymers

Finally, the mechanical properties were investigated for the self-healing polyurethanes. The average ultimate tensile stresses

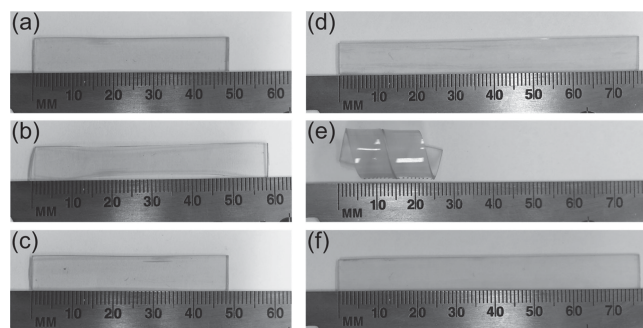


**Figure 5.** Images of 1.5DA1T films show a) permanent shape (48.6 mm × 8.73 mm × 1.08 mm), b) temporary shape after deforming and fixing, c) permanent shape after recovering, d) permanent shape (76.5 mm × 8.6 mm × 1.06 mm), e) spiral temporary shape, and f) recovered permanent shape

and the Young's modulus from 12 specimens were 76.8 MPa and 2.86 GPa for 1DA1T and 87.3 MPa and 2.48 GPa for 1.5DA1T, respectively. They are comparable to composites grade epoxy but the ultimate tensile strain of 1DA1T is much larger than epoxy. This indicates that 1DA1T and 1.5DA1T polymers still exhibit elastomeric behavior as a result of the TEA and HDI polyurethanes even after adding DA crosslinking to the polymer. For fracture toughness, a total of 6 specimens of each polymer were tested and 1.43 MPa for 1DA1T and 1.06 MPa were obtained. Both average fracture toughness are more than that of an epoxy. In **Table 2**, all data are listed and the standard deviations of each property are also shown. These data were compared to composite grade epoxy since the developed polyurethane was studied as a possible substitute to epoxy fractions in structural composites, also generally known as polymer matrix composites.

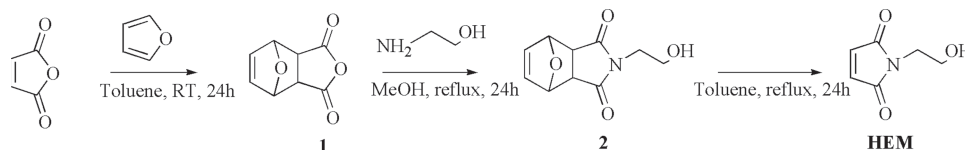
## 3. Conclusion

This work has developed polymers combining two functionalities, self-healing polymers and shape memory polymers. This eliminates the need to apply an external force to close a crack during the healing process. The polyurethane backbone created excellent mechanical properties comparable to epoxy while allowing the DA monomers to link to the main polymer chains and achieve healing as well as its shape memory ability. The healing efficiencies calculated using maximum loads from CT testing confirmed that repeated healing without external pressure was possible with only slight loss efficiency.

**Table 2.** Comparison of mechanical properties between 1DA1T, 1.5DA1T, and epoxy.

Property	1DA1T	Standard Deviation	1.5DA1T	Standard Deviation	Epoxy
Ultimate tensile strength [MPa]	76.8	8.2	87.8	7.6	35–130 <sup>20</sup>
Ultimate tensile strain [%]	30.5	23.5	5.4	2.8	2–5 <sup>21</sup>
Young's modulus [GPa]	2.37	0.25	2.57	0.17	2–6 <sup>20</sup>
Glass transition temperature [°C]	42.4	2.06	45.6	3.77	50–250 <sup>20</sup>
Fracture toughness [MPa·√m]	1.43	0.14	1.06	0.04	0.65 <sup>22a)</sup>

<sup>a)</sup>Epoxy resin (L135i) with an amine hardener (H137i).



**Scheme 1.** Three steps synthesis of *N*-(2-hydroxyethyl) maleimide.

## 4. Experimental Section

### 4.1. Syntheses

**Materials:** Furfuryl alcohol (Acros Organics), hexamethylene diisocyanate (Acros Organics), and triethanolamine (Sigma-Aldrich) are used as received. Maleimide monomers, *N*-(2-hydroxyethyl)-maleimide (HEM), is prepared with Diels–Alder and retro Diels–Alder cycloaddition through a three steps process as shown in **Scheme 1**. Heath et al.'s method<sup>[17]</sup> is mainly used but modified slightly. For the HEM synthesis, maleic anhydride (Alfa Aesar), furan (Acros Organics), ethanolamine (Acros Organics), methanol (Fisher Chemical) and toluene (Fisher Chemical) were used as received.

**4,10-Dioxatricyclo[5.2.1.0<sup>2,6</sup>]dec-8-ene-3,5-dione (1):** Maleic anhydride (30 g, 305.94 mmol) and furan (21 g, 308.51 mmol) are mixed and stirred in toluene (300 mL) at room temperature for 24 h. Furan is added slightly more than maleic anhydride to make sure all maleic anhydride are crosslinked with furan. After 24 hours, a fine white solid powder is precipitated and the mixture is vacuum filtered and dried to obtain the product (1). Unreacted furan is filtered during the vacuum filtration process and a further purification step is not necessary (yield 85.6%). mp 123 °C; <sup>1</sup>H NMR (300 Hz, DMSO-*d*<sub>6</sub>) δ 6.59 (s, 2H), 5.36 (s, 2H), 3.32 (s, 2H) ppm; <sup>13</sup>C NMR (300 Hz, DMSO-*d*<sub>6</sub>) δ 171.98, 137.30, 82.11, 49.53 ppm.

**4-(2-Hydroxy-ethyl)-10-oxa-4-aza-tricyclo[5.2.1.0<sup>2,6</sup>]dec-8-ene-3,5-dione (2):** 4,10-Dioxatricyclo[5.2.1.0<sup>2,6</sup>]dec-8-ene-3,5-dione (1) (30 g, 180.58 mmol) and methanol (60 mL) are added to a flask and the mixture is kept in an ice bath for 15 min. Ethanolamine (11.04 g, 180.75 mmol) is mixed well with methanol (5 mL) and this mixture is slowly added over 30 min to the flask in the ice bath under stirring. The final mixture is then kept in the ice bath for 30 min and then at room temperature for an additional 30 min. The product (1) is dissolved completely into methanol while adding ethanolamine. Then, the solution is refluxed for 24 h. Afterwards, the solution is cooled down and a slightly yellowish solid powder is crystallized. This powder is then vacuum filtered and dried (yield 46.6%). mp 142 °C; <sup>1</sup>H NMR (300 Hz, DMSO-*d*<sub>6</sub>) δ 6.53 (s, 2H), 5.10 (s, 2H), 4.74 (br, 1H), 3.40 (br, 4H), 2.90 (s, 2H) ppm; <sup>13</sup>C NMR (300 Hz, DMSO-*d*<sub>6</sub>) δ 176.93, 136.89, 80.73, 57.73, 47.57, 41.06 ppm.

***N*-(2-Hydroxyethyl)-maleimide (HEM):** 4-(2-Hydroxyethyl)-10-oxa-4-aza-tricyclo[5.2.1.0<sup>2,6</sup>]dec-8-ene-3,5-dione (2) (30 g) is refluxed in toluene (180 mL) for over 24 h until it is completely cleaved. To confirm the cleaving, NMR was used and 6.520 ppm and 5.104 ppm should disappear once furan is removed from 4-(2-Hydroxyethyl)-10-oxa-4-aza-tricyclo[5.2.1.0<sup>2,6</sup>]dec-8-ene-3,5-dione (2). The solution is cooled down and white powders are crystallized and they can be collected by the vacuum filtration. (yield 83.02%); mp 75 °C; <sup>1</sup>H NMR (300 Hz,

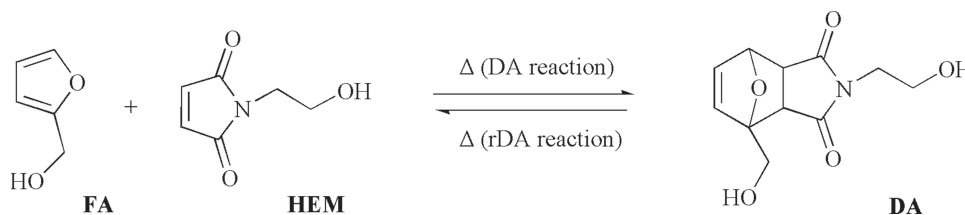
DMSO-*d*<sub>6</sub>) δ 6.97 (s, 2H), 4.80 (br, 1H), 3.44 (br, 4H) ppm; <sup>13</sup>C NMR (300 Hz, DMSO-*d*<sub>6</sub>) δ 171.53, 134.88, 58.37, 40.38 ppm.

**Pre-crosslinking DA Adducts (DA):** To make sure that all DA adducts are completely crosslinked before cracking, HEM and furfuryl alcohol (FA) are precrosslinked by using the DA reaction before the polymerization step as shown in **Scheme 2**. For HEM and FA, each monomer is added into toluene with a 1:1 molar ratio and then the mixtures are heated to 75 °C under stirring for 12 h, then a light yellowish precipitation is observed. The product is then vacuum filtered and washed twice with ether (yield 90.09%). mp 109 °C; <sup>1</sup>H NMR (300 Hz, DMSO-*d*<sub>6</sub>) δ 6.52 (br, 2H), 5.07 (s, 1H), 4.92 (br, 1H), 4.75 (br, 1H), 4.01 (d, 1H), 3.71 (d, 1H), 3.41 (s, 4H), 3.03 (d, 1H), 2.89 (d, 1H) ppm; <sup>13</sup>C NMR (300 Hz, DMSO-*d*<sub>6</sub>) δ 176.85, 175.40, 138.53, 136.91, 92.07, 80.63, 59.40, 57.74, 50.39, 48.21, 41.00 ppm.

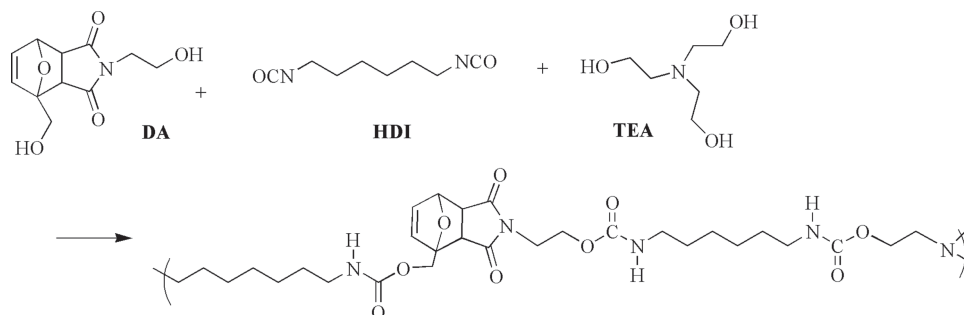
**Polymers:** Maleimide moieties usually are solid at room temperature and have high melting points compared to the rest of the monomers (i.e., FA, TEA, and HDI). A bulk or film polymerization method that used by other researchers<sup>[3,4,23]</sup> is to mix and dissolve the monomers into a solvent and then let the solvent evaporate slowly to acquire the polymer products. However, if a solvent is not completely removed during this process, the material properties of a polymer could end up changing. In order to avoid this potential problem, in this work, the solid DA monomers are heated and melt at 105 °C and then mixed the hot resin monomer with the rest of monomers (TEA and HDI) at the same temperature. Then, the mixtures are poured into the Teflon mold and place the mold into the preheated oven to 100 °C under nitrogen condition. The temperature is increased to 125 °C and stayed for 2 h and then decreased to 90 °C over 1 h and kept for 2 h. After that, the oven is cooled down to 70 °C over 1 h and kept for 2 h and finally the polymers are cooled down in oven slowly to room temperature. The polymerization and cooling temperature profile is similar to the healing process that is designed to maximize the number of crosslinked condition in polymer when the reaction is done. This polymerization process with the HEM monomer is shown in detail (see **Scheme 3**).

### 4.2. Thermal Analysis of the Polymers

A thermogravimetric analysis (TGA), TA Q50, was utilized to check the polymer decomposition temperature. The TGA data also can be used to anticipate the maximum temperature for the following DSC test. Each sample with a mass of approximately 15 mg was placed in a platinum pan first. The temperature was increased from 20 °C up to 600 °C with a heating rate of 20 °C/min under a nitrogen atmosphere. The balance purge flow and sample purge flow of nitrogen were set at 40 mL/min and 60 mL/min, respectively. TGA data can be seen in Figure S9 in the Supporting Information.



**Scheme 2.** A schematic of the precrosslinked FA and HEM.



**Scheme 3.** A schematic of the polymerization reaction with DA, TEA, and HDI monomers.

A differential scanning calorimetry (DSC), TA Q20, was used for thermal analyses such as the glass transition, crosslinking, and cleaving temperatures of each polymer. For testing, each polymer sample was preheated at 130 °C for 2 h and then quenched in an ice bath. This procedure was necessary to promote cleaved bonds in the polymer structures so that the crosslinking transition which is observed at lower temperature can be shown clearly. Then, samples that weighted between 10 mg and 15 mg were placed in standard Tzero aluminium pan. Two aluminium pans with and without samples were put on each sensor platform. The temperature ranges for DSC testing were from −10 °C to 160 °C under the nitrogen atmosphere and the sample purge flow rate of nitrogen was set at 50 mL/min. In more detail, a sample was cooled down to an equilibration temperature of −10 °C for 2 min and linearly heated up to 160 °C with a ramping rate of 10 °C/min. After data acquisition, all data were analyzed by using “TA Universal Analysis” software offered by the TA Company. The average glass transition temperatures, crosslinking temperatures and cleaving temperatures of 6 specimens of 1DA1T and 1.5DA1T polymers are reported in Table 1.

### 4.3. Reversibility of Self-Healing Mechanism

In order to study the reversibility of the DA reaction and retro DA reaction, variable temperature proton nuclear magnetic resonance (VT NMR) was utilized to observe new  $\sigma$  bond peaks (i.e., 6.52 ppm and 5.18 ppm) in the chemical shifts. An Inova 2 500 MHz NMR instrument was used and the deuterated dimethyl sulfoxide (DMSO- $d_6$ ) was used for all NMR specimens as a solvent. A specimen was heated up with an internal heating function of the Inova 2 instrument and cooled down with an external liquid nitrogen cooling system in air. Precrosslinked HEM and FA monomers in dimethyl sulfoxide- $d_6$  solvent were used and all spectra were acquired at different temperatures. The samples were kept at 140 °C for 30 min for the cleaving process and then cooled down to 80 °C for 120 min for the crosslinking DA reaction. Then, the same temperature and time profiles were used again to confirm the reversibility of crosslinking and cleaving reactions. The temperatures, 80 °C and 140 °C, were chosen since it was believed that these temperatures were in the range of the crosslinking and cleaving reactions, and the peaks were scanned every 10 min to study the reaction kinetics. These time and temperature data were used later to design the healing process.

### 4.4. Healing Efficiency

In order to calculate the healing efficiency, the fracture load was measured with compact tension (CT) testing. This was conducted using an Instron 5969 at room temperature. The ASTM D 5045 standard was followed with slight modifications in dimensions as shown in Figure 3a and the constant opening rates for all tests before and after each healing process were used (3 mm/min for 1DA1T and 1 mm/min for 1.5DA1T). The opening rates were adjusted to initiate crack propagation without deforming the samples, avoid crazing and to ensure the crack stops

at the resting hole. Under the ASTM D 5045 standard, at least five specimens are required and averaged to obtain the values. Thus, 6 specimens were tested for 1DA1T and 8 specimens were examined for 1.5DA1T. More 1.5DA1T specimens were test to achieve better statistical stability since the initial 6 values were varied. The standard deviations of each polymer set were also calculated and shown as error bars in Figure 3b.

### 4.5. Shape Memory Characterization

In addition to the self-healing properties of the polyurethane, the shape memory properties were also confirmed. The tests to verify the recovery capability in two different directions under free-strain were undertaken to evaluate the shape memory property. One newly synthesized film with dimensions of 48.6 mm  $\times$  8.73 mm  $\times$  1.08 mm was heated at 100 °C for 5 min, stretched in longitudinal direction, and cooled down to room temperature in order to fix the temporary shape. Then, the film was re-heated to 100 °C for 5 min to let the permanent shape recover. Another film with dimensions of 76.5 mm  $\times$  8.6 mm  $\times$  1.06 mm was used to show the spiral shape memory property. Similar to the other sample, it was heated to 100 °C for 5 min, coiled, and cooled down to room temperature to fix the temporary shape. Then, to recover the permanent shape the film was re-heated to 100 °C for 5 min.

### 4.6. Mechanical Properties

The dimensions of the ASTM 638 Type V sample were tested and a total of 12 flat specimens of each 1DA1T and 1.5DA1T were prepared to measure the ultimate tensile strength, strain, and Young's modulus. All tensile tests were done at room temperature and the opening rate of 5 mm/min was used. In addition, the maximum loads at fracture from a compact tension test were obtained to calculate the fracture toughness. The test conditions, procedures and dimensions of the specimen for the CT test were satisfied by the ASTM D 5045 standards. Each of 6 specimens was tested at room temperature on an Instron 5969 at an opening rate of 5 mm/min.

## Supporting Information

Supporting Information is available from the Wiley Online Library or from the author.

## Acknowledgements

The authors gratefully acknowledge the support from the Army Research Office (Award #: W911NF-12-1-0014) and would also like to

thank Mr. M. H. Malakooti for all discussion and help related to the mechanical testing.

Received: January 27, 2014

Revised: March 27, 2014

Published online: May 30, 2014

- [1] a) S. R. White, N. Sottos, P. Geubelle, J. Moore, M. R. Kessler, S. Sriram, E. Brown, S. Viswanathan, *Nature* **2001**, 409, 794; b) E. N. Brown, N. Sottos, S. R. White, *Exp. Mech.* **2002**, 42, 372; c) B. Blaiszik, N. Sottos, S. White, *Compos. Sci. Technol.* **2008**, 68, 978; d) S. H. Cho, S. R. White, P. V. Braun, *Adv. Mater.* **2009**, 21, 645; e) B. Blaiszik, S. Kramer, S. Olugebefola, J. S. Moore, N. R. Sottos, S. R. White, *Ann. Rev. Mater. Res.* **2010**, 40, 179.
- [2] a) C. Dry, *Compos. Struct.* **1996**, 35, 263; b) R. Trask, G. Williams, I. Bond, *J. R. Soc. Interface* **2007**, 4, 363; c) G. Williams, R. Trask, I. Bond, *Compos. Part A: Appl. S.* **2007**, 38, 1525; d) J. W. Pang, I. P. Bond, *Compos. Sci. Technol.* **2005**, 65, 1791; e) M. Keller, N. Sottos, *Exp. Mech.* **2006**, 46, 725; f) S. Kim, S. Lorente, A. Bejan, *Jpn. J. Appl. Phys.* **2006**, 100, 063525; g) K. Wang, S. Lorente, A. Bejan, *J. Phys. D: Appl. Phys.* **2006**, 39, 3086.
- [3] X. Chen, M. A. Dam, K. Ono, A. Mal, H. Shen, S. R. Nutt, K. Sheran, F. Wudl, *Science* **2002**, 295, 1698.
- [4] X. Chen, F. Wudl, A. K. Mal, H. Shen, S. R. Nutt, *Macromolecules* **2003**, 36, 1802.
- [5] a) R. Gheneim, C. Perez-Berumen, A. Gandini, *Macromolecules* **2002**, 35, 7246; b) A. Amalin Kavitha, N. K. Singha, *J. Polym. Sci. A1* **2007**, 45, 4441; c) Y. Zhang, A. A. Broekhuis, F. Picchioni, *Macromolecules* **2009**, 42, 1906; d) C. Toncelli, D. C. De Reus, F. Picchioni, A. A. Broekhuis, *Macromol. Chem. Phys.* **2012**, 213, 157.
- [6] O. Diels, K. Alder, *Liebigs. Ann. Chem.* **1928**, 460, 98.
- [7] B. Rickborn, in *Organic Reactions*, John Wiley & Sons, Inc., New York, USA **1998**.
- [8] D. L. Reger, S. R. Goode, D. W. Ball, in *Chemistry: Principles and Practice*, Thomson Brooks/Cole, Belmont, USA **2009**.
- [9] T. C. Mauldin, M. R. Kessler, *Int. Mater. Rev.* **2010**, 55, 317.
- [10] A. Lendlein, S. Kelch, *Angew. Chem. Int. Edit.* **2002**, 41, 2034.
- [11] A. Lendlein, A. M. Schmidt, R. Langer, *Proc. Natl. Acad. Sci. USA* **2001**, 98, 842.
- [12] M. Behl, A. Lendlein, *Mater. Today* **2007**, 10, 20.
- [13] T. S. Wilson, J. P. Bearinger, J. L. Herberg, I. J. E. Marion, W. J. Wright, C. L. Evans, D. J. Maitland, *J. Appl. Polym. Sci.* **2007**, 106, 540.
- [14] E. D. Rodriguez, X. Luo, P. T. Mather, *ACS Appl. Mater. Interfaces* **2011**, 3, 152.
- [15] X. Luo, P. T. Mather, *ACS Macro Lett.* **2013**, 2, 152.
- [16] C. Liu, H. Qin, P. T. Mather, *J. Mater. Chem.* **2007**, 17, 1543.
- [17] W. H. Heath, F. Palmieri, J. R. Adams, B. K. Long, J. Chute, T. W. Holcombe, S. Zieren, M. J. Truitt, J. L. White, C. G. Willson, *Macromolecules* **2008**, 41, 719.
- [18] S. Burattini, B. W. Greenland, D. Chappell, H. M. Colquhoun, W. Hayes, *Chem. Soc. Rev.* **2010**, 39, 1973.
- [19] E. B. Murphy, E. Bolanos, C. Schaffner-Hamann, F. Wudl, S. R. Nutt, M. L. Auad, *Macromolecules* **2008**, 41, 5203.
- [20] M. W. Hyer, S. R. White, in *Stress Analysis of Fiber-Reinforced Composite Materials*, McGraw-Hill Companies, Inc., New York, USA **1998**, p.26.
- [21] I. M. Daniel, O. Ishai, I. M. Daniel, I. Daniel, in *Engineering Mechanics of Composite Materials*, 1<sup>st</sup> Ed, Oxford University Press, New York, USA **2006**.
- [22] F. H. Gojny, M. H. G. Wichmann, B. Fiedler, K. Schulte, *Compos. Sci. Technol.* **2005**, 65, 2300.
- [23] a) T. A. Plasided, S. Nemat-Nasser, *Acta Mater.* **2007**, 55, 5684; b) J. Zhang, Y. Niu, C. Huang, L. Xiao, Z. Chen, K. Yang, Y. Wang, *Polym. Chem.* **2012**, 3, 1390; c) H. Weizman, C. Nielsen, O. S. Weizman, S. Nemat-Nasser, *J. Chem. Educ.* **2011**, 88, 1137; d) N. Yoshie, S. Saito, N. Oya, *Polymer* **2011**, 52, 6074.